

Studies on Through Flow Drying. I. Heat and Mass Transfer between Fluid and Solids in Packed Bed

By

Masakatsu HIRAOKA* and Ryozo TOEI**

(Received October 26, 1961)

The mechanisms of through flow drying were investigated experimentally and theoretically. Part I of this paper deals with heat and mass transfer during the constant drying period. The experimental data were obtained by measuring the rate of evaporation of water into a stream of air from wetted granules and packings during the constant drying rate period. The drying rates of a single layer of wetted porcelain particles packed between two layers of dry glass spheres were measured and those of random packed beds also were obtained. From a comparison of the transfer data with a single layer and with packed beds, the characteristic constants of the packings were determined and a correlation of the transfer coefficients was obtained.

Furthermore, the discussion is extended to considerations of transfer phenomena in fluidized beds.

1. Introduction

At present, through flow dryers are being used widely for drying granular materials in the final process of chemical industries. Through flow dryers operate on the principle of blowing hot air through a permeable bed of wet material in the dryer. Drying rates are high because of the large area exposed and the short distance of travel for the internal moisture. In order to predict the rate of through flow drying, it is necessary to understand the phenomena of heat and mass transfer between fluid and particles in a packed bed.

Many studies of the heat and mass transfer coefficients between fluid and solids in packed beds have been done, but the published experimental data are still relatively meager when compared with the extensive data available on transfer phenomena in conduits. There is especially, little information on transfer data for the case where the fluid is a gas.

Gamson, Thodos and Hougen³⁾, and Wilke and Hougen¹⁰⁾ developed a generalized correlation of heat and mass transfer coefficients between fluids and solids

* Department of Sanitary Engineering

** Department of Chemical Engineering

in packed beds. Their experimental data were obtained by measuring the rate of evaporation of water into a stream of air from wetted granules and packings during the constant drying rate period. Hurt⁴⁾, and Resnick and White⁸⁾ presented mass transfer data for the evaporation of naphthalene into a stream of flowing air. The naphthalene results did not agree with each other or with the data of Hougen and coworkers. Denton²⁾ measured the rates of heat transfer between electrically heated packed spheres and air. Baumeister *et al.*¹⁾ obtained data on heat transfer by measuring the heat transferred from a packed steel ball heated by a dielectric generator to air. Satterfield⁹⁾ discussed a system in which the vapor of hydrogen peroxide is passed through a bed of catalytic spheres. McCune and Wilhelm⁵⁾ reported data on mass transfer between granular solids and flowing liquids. W. E. Ranz⁶⁾ developed a method of analysis based on the properties of a single particle to estimate and characterize the transfer rates of packed beds. He assumed that a major contribution to the total heat and mass transfer occurs on the forward faces of the particle; in the packed bed, each particle is located in front of a jet formed by the three particles preceding it and most of the transfer occurs at the point where the jet impinges upon the forward face of the particle. He analysed the relationship between the velocity through the jet and the velocity through the empty column for a model of packed bed, and derived an expression for the transfer rate in a model bed by taking $10.73 Re_0$ instead of the Reynolds number Re_0 in the equation for the transfer rate of a single sphere in a fluid stream.

In this report, the data of heat and mass transfer between fluid and solid were summarized and correlated in accordance with the method of W. E. Ranz. Experimental data were obtained by measuring the rates of the constant drying period of packed beds.

2. Experimental apparatus and procedure

The flow set for the experimental apparatus is shown in Fig. 1 and the details of the vessel are illustrated in Fig. 2. The inside diameter of the vessel made from pyrex glass was 8 cm and its height was about 30 cm. The vessel consists of a double cylinder whose annular space is in vacuum to prevent heat loss. The upper part of the vessel, equipped with an internal screen support for the bed of spheres, served as a drying chamber and is joined to the box in the lower part filled with mercury. Rapid weighing of the drying chamber was made possible by lifting the upper part from the mercury box and balancing it with a chemical balance, equipped with a magnet to stop vibration. The mercury box acted as a flexible joint and was effective as a tight seal at the low pressures

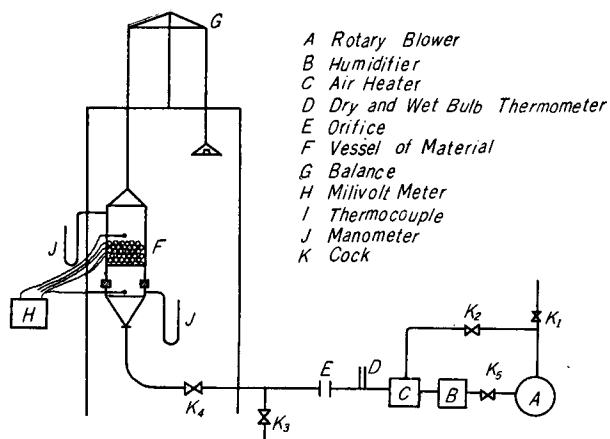


Fig. 1.

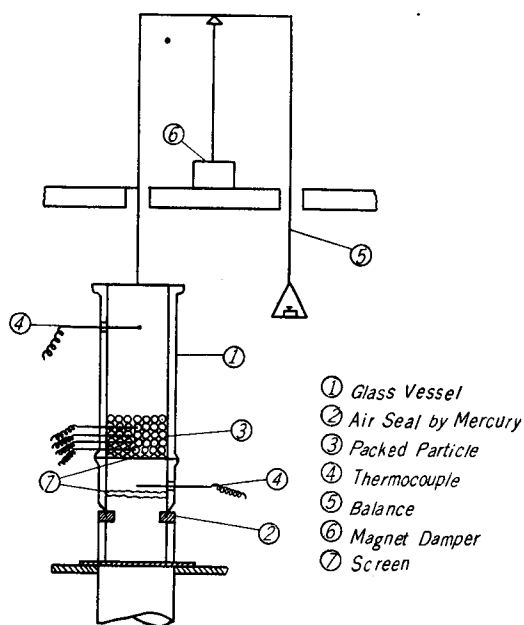


Fig. 2.

used in the experimental work. Quick opening valves K_3 , K_4 were installed in the gas feed line and in a by-pass connection just in front of the vessels in order to introduce or cut off instantaneously the gas flow to the vaporization chamber. Air was supplied from the blower and maintained at constant humidity and temperature by flowing through the air humidifier and air heater. Air flow

rate was measured by an orifice installed at point *E* in the horizontal pipe line from the blower. The spheres permanently equipped with thermocouples were regularly distributed at equal intervals at the centre of the cross section of the bed and their surface temperatures were measured. Temperatures of the air at the inlet and outlet of the drying chamber were also measured by thermocouples inserted into the vessel. Thermocouples were connected with the millivoltmeter by using a very fine wire of platinum of 0.06 mm diameter and about 10 cm length in the middle of the connecting line and were able to be weighed together with the drying chamber. The blower was stopped and the drying chamber was weighed at the 2 min. intervals through out a run. The time required for weighing the drying chamber seldom exceeded 20 sec. The sizes of the porous spherical and cylindrical packings for the experiment are summarized in Table 1.

Table 1. Size of particle

Material	Diameter D_p (m)	Volume (m^3)	Surface Area (m^2)
Porcelain (Sphere)	13.29×10^{-3}	1.229×10^{-6}	5.534×10^{-4}
"	11.29×10^{-3}	7.502×10^{-7}	4.002×10^{-4}
"	9.43×10^{-3}	4.510×10^{-7}	2.795×10^{-4}
"	7.464×10^{-3}	2.179×10^{-7}	1.761×10^{-4}
"	4.807×10^{-3}	5.841×10^{-8}	7.251×10^{-5}
Activated Alumina (sphere)	4.873×10^{-3}	6.056×10^{-8}	7.456×10^{-5}
"	4.257×10^{-3}	4.051×10^{-8}	5.708×10^{-5}
"	3.678×10^{-3}	2.596×10^{-8}	4.253×10^{-5}
"	1.857×10^{-3}	3.351×10^{-9}	1.083×10^{-5}
"	1.498×10^{-3}	1.763×10^{-9}	7.062×10^{-6}
"	1.142×10^{-3}	7.823×10^{-10}	4.107×10^{-6}
"	0.994×10^{-3}	5.131×10^{-10}	3.102×10^{-6}
Porcelain (cylinder)	$D_{pe} = 14.6 \times 10^{-3}$	1.27×10^{-6}	66.8×10^{-5}
"	$D_{pe} = 7.84 \times 10^{-3}$	1.91×10^{-7}	19.25×10^{-5}
Activated Alumina (Tablet)	$D_{pe} = 7.8 \times 10^{-3}$	2.16×10^{-7}	2.07×10^{-4}

The drying experiments were performed for two methods of packings. At first, the drying rates of a single layer of wetted porcelain particles between two layers of dry glass spheres were measured, and then the drying rates for a random packed bed of 4-5 cm height were also obtained. All runs were so performed that the effluent air was below the point of saturation. Unless the effluent air is below the point of saturation, the driving force for transfer can not be properly expressed in the basic rate equation for the entire bed.

3. Experimental results

The experimental procedure described above, yields drying curves relating

reduced weight and time from which the constant drying rate values are determined. The heat and mass transfer coefficients are then calculated from the basic rate equation applied to transfer across a gas film.

$$\left(\frac{dw}{d\theta}\right)_c = ha(\Delta t)_{lm}V/\gamma_w = k_{ca}(\Delta H)_{lm}V \quad (1)$$

In the calculations with equation (1), it was assumed that the vaporization in the constant rate period takes place at the wet bulb temperature and that the surface temperatures of the particles are also at the wet-bulb temperature. In the experiments, the readings of the thermocouples inserted in particles of large diameter were near the wet-bulb temperature, but it was difficult to measure

Table 2. Experimental and Calculated Data of Heat and Mass transfer of Singlelayer of Particle

Run	t_1 (°C)	H (kg/kg)	G (kg/hrm ²)	t_w (°C)	$\frac{dW}{d\theta}$ (kg/hr)	h (kcal/hrm ²)	jh	D_p (m)	A_p (m ²)	m (%)	
3	36	0.017	4590	26	0.034	120	0.0903	7.46×10^{-3}	0.95×10^{-3}	93	
4	32.5	0.017	5650	25	0.030	143	0.0878	" "	" "	92	
2	36.3	0.017	4070	26	0.0315	113	0.0962	" "	" "	89	
6	36.2	0.018	3200	26.2	0.027	93	0.1005	" "	" "	96	
10	34.3	0.017	3550	25.3	0.029	102	0.0994	4.807×10^{-3}	0.88×10^{-3}	252	
9	36.0	0.017	4130	26.0	0.0365	119	0.100	" "	" "	245	
11	34.3	0.017	4580	25.3	0.0335	121.5	0.0917	" "	" "	245	
18	30.0	0.019	2920	25.6	0.0140	102	0.1210	" "	" "	248	
17	29.6	0.018	3090	25.0	0.0140	107	0.104	3.678×10^{-3}	" "	387	
12	30.0	0.019	3820	25.5	0.0150	104	0.0940	4.807×10^{-3}	" "	256	
13	30.0	0.019	5670	25.5	0.0215	153	0.0933	" "	" "	250	
14	30.0	0.019	4500	25.5	0.0181	127	0.0900	" "	" "	253	
	R_{e0}	R_{e2}	N_u	$Nu-2/Pr^{2/3}$	$Nu-2/Pr^{1/3}$	H_w	k_g	S_c	S_{ch}	$S_{ch-2}/S_c^{1/3}$	jd
3	507	2920	43.3	48.2	44.6	0.0210	520	0.635	42.3	46.9	0.0836
4	630	3320	52.0	58.3	54	0.0201	598	0.635	48.8	54.4	0.0782
2	450	2380	40.8	45.2	41.9	0.0210	502	0.635	41.0	45.3	0.0913
6	353	1850	33.6	36.8	34.1	0.0216	434	0.635	31.8	34.7	0.0902
10	253	1440	23.8	25.4	23.5	0.02045	461	0.625	24.2	25.8	0.0960
9	294	1680	27.8	29.7	27.8	0.0210	513	0.635	27.0	29.0	0.0905
11	326	1870	28.1	30.7	28.2	0.02045	540	0.635	28.4	30.7	0.0873
18	208	1180	23.8	25.4	23.5	0.02080	434	0.635	22.8	24.2	0.110
17	168	947	19.2	20.0	18.5	0.0201	405	0.635	16.3	16.7	0.0970
12	272	1190	24.2	25.9	24.1	0.0207	477	0.635	25.1	26.8	0.0924
13	404	2300	35.6	39.1	36.2	0.0207	625	0.635	32.9	36.0	
14	321	1830	29.6	32.2	29.8	0.0207	581	0.635	30.7	33.4	0.0948

surface temperatures with particles of diameters less than 3 mm.

(1) Heat and mass transfer with a single layer of porous spheres. As mentioned previously, the heat and mass transfer coefficients with a single layer of spheres in fluid flow through a packed bed were obtained by measuring the drying rate of a single layer of wetted particles between two layers of dry glass spheres. The experimental data and calculated results are summarized in Table 2. Fig. 3 shows plots in the form of $(Nu-2)/(Pr)^{1/3}$ or $(Sh-2)/(Sc)^{1/3}$ versus Reynolds number Re_p based on the average velocity through the interstices of a single layer of particles exposed to the stream.

From Fig. 3, the experimental data may be expressed by the following equation.

$$\left. \begin{aligned} Nu &= 2.0 + 0.113 (Re_p)^{0.75} (Pr)^{1/3} \\ Sh &= 2.0 + 0.113 (Re_p)^{0.75} (Sc)^{1/3} \end{aligned} \right\} \quad (2)$$

It was assumed that a sphere in a packed bed has the value of 2.0 for Nusselts number when Reynolds number approaches zero, the same as for a single sphere in a flowing stream. Equation (2) does not agree with the equation of heat and mass transfer for single particles obtained by Ranz and Marshall⁷.

(2) Heat and mass transfer in packed beds.

The experimental data and calculated results of heat and mass transfer of packed beds are summarized in Table 3 and also plotted in Fig. 3 in the form of $(Nu-2)/(Pr)^{1/3}$, $(Sh-2)/(Sc)^{1/3}$ versus Reynolds number Re_0 based on the fluid velocity v_0 through the empty column.

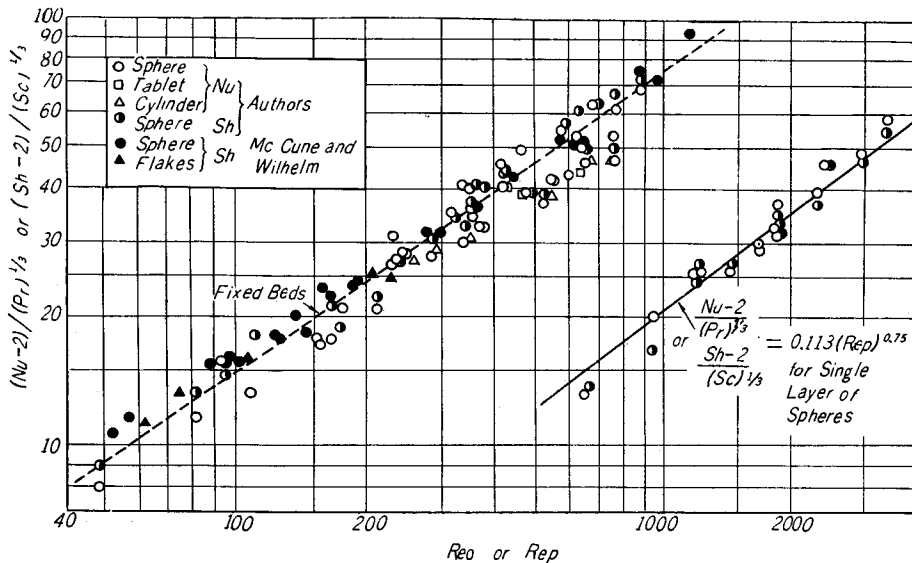


Fig. 3.

By comparison of equation (2) with the transfer data for packed beds, the values of K , the ratio of the fluid velocity through the interstices of packings to the fluid velocity through the empty column were evaluated and plotted on semilog paper as shown in the right part of Fig. 4. The values of K varied between 5.5 and 7.2. The effect of the sphericity of the particles on the value of K could not be recognized from Fig. 4. Heat and mass transfer data in the packed beds were correlated as follows by using the values of K .

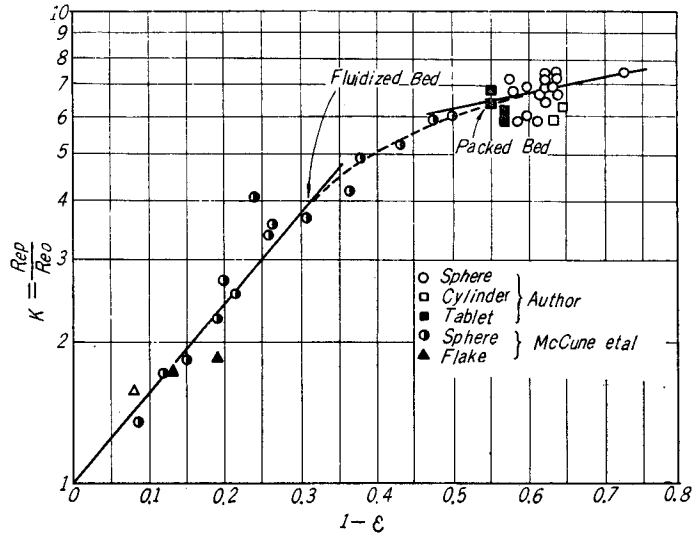


Fig. 4.

$$\left. \begin{aligned} Nu &= 2.0 + (KRe_0)^{0.75} (Pr)^{1/3} \\ Sh &= 2.0 + (KRe_0)^{0.75} (Sc)^{1/3} \end{aligned} \right\} \quad (3)$$

where

$$\begin{aligned} K &= 4.2 e^{0.75(1-\epsilon)} \\ 50 &< Re_0 < 3000 \end{aligned}$$

4. Discussion

(1) Comparison with the results of other investigators

In order to compare results with those of other investigators, the data of heat and mass transfer were plotted on Fig. 5 and Fig. 6 in the form of j -factor versus Re_0 along with the results of other investigators. The expressions obtained for the j -factor are as follows.

$$\left. \begin{aligned} j_h &= 1.20 (Re_0)^{-0.45} & Re_0 < 140 \\ j_h &= 0.60 (Re_0)^{-0.305} & Re_0 > 140 \end{aligned} \right\} \quad (4)$$

Table 3. Experimental and Calculated Date of Heat

	t_1 (°C)	H_1 (kg/kg)	t_w (°C)	G ($\frac{kg}{hrm^2}$)	C_H ($\frac{kcal}{kg^{\circ}C}$)	$\frac{dW}{d\theta}$ (kg/hr)	h ($\frac{kcal}{hrm^2^{\circ}C}$)	jh	D_p (m)	L (m)
Run 109 (Activated Alumina Tablet)	55	0.013	28.1	5650	0.246	0.25	135	0.0831	7.78×10^{-3}	22×10^{-3}
110 "	55.2	0.012	27.8	5520	0.246	0.218	126.5	0.0702	"	21×10^{-3}
111 "	45.7	0.012	25.4	4830	0.246	0.153	109	0.0780	"	22×10^{-3}
112 "	40.3	0.013	24.7	4170	0.246	0.1002	101.0	0.0843	"	16×10^{-3}
116 "	48.0	0.011	25.3	3730	0.246	0.1315	105	0.0988	"	17×10^{-3}
Run 97 (Porcelain Cylinder (small))	39.3	0.0100	22.2	2475	0.2445	0.0714	72.1	0.1037	7.83×10^{-3}	17×10^{-3}
102 "	39.3	0.0106	22.7	2944	0.245	0.0840	77.7	0.0932	"	18×10^{-3}
100 "	37.3	0.011	22.4	2110	0.245	0.0570	73.7	0.112	"	16×10^{-3}
95 "	40.2	0.009	22.0	3040	0.244	0.0972	89.9	0.103	"	18×10^{-3}
101 (Porcelain Cylinder (large))	39.3	0.0105	22.5	3585	0.245	0.0768	64.7	0.0633	14.2×10^{-3}	30×10^{-3}
99 "	38.6	0.0108	22.5	3555	0.245	0.0702	73.8	0.0725	"	31×10^{-3}
98 "	38.0	0.0100	22.0	2420	0.2445	0.0510	53.9	0.0788	"	26×10^{-3}
94 "	41.3	0.0095	22.4	2962	0.2443	0.0798	64.2	0.0769	"	32×10^{-3}
Run 93 (Porcelain sphere)	42.0	0.0095	22.9	4560	0.244	0.1008	100.0	0.0768	13.29×10^{-3}	33×10^{-3}
91 "	39.5	0.0090	21.8	2875	0.244	0.0768	92.0	0.1139	7.46×10^{-3}	20×10^{-3}
90 "	38.0	0.0100	21.9	3242	0.245	0.0984	131.7	0.1481	4.807×10^{-3}	15×10^{-3}
88 "	39.0	0.0101	22.2	2800	0.245	0.0756	86.3	0.1078	11.29×10^{-3}	37×10^{-3}
87 "	42.0	0.0100	23.1	3760	0.245	0.1134	90.9	0.0855	11.29×10^{-3}	44×10^{-3}
86 "	41.8	0.0101	22.9	2941	0.245	0.0882	89.0	0.0798	13.29×10^{-3}	34×10^{-3}
85 "	40.7	0.0100	22.8	3205	0.245	0.1014	96.5	0.1065	7.464×10^{-3}	30×10^{-3}
83 "	40.9	0.0102	22.9	3300	0.245	0.0702	75.3	0.0807	13.29×10^{-3}	34×10^{-3}
82 "	37.3	0.00999	21.8	2694	0.244	0.0672	88.2	0.1169	11.29×10^{-3}	37×10^{-3}
81 "	39.9	0.0115	23.5	3500	0.245	0.0744	92.0	0.0920	13.29×10^{-3}	38×10^{-3}
80 "	39.3	0.0105	22.4	3120	0.245	0.0903	110	0.1248	7.464×10^{-3}	34×10^{-3}
79 "	38.6	0.0109	22.9	3460	0.245	0.0852	98.8	0.100	11.29×10^{-3}	38×10^{-3}
77 "	39.7	0.0100	22.2	2300	0.245	0.0596	66.3	0.102	13.29×10^{-3}	37×10^{-3}
76 "	39.7	0.0095	22.1	2223	0.245	0.05676	58.2	0.0924	11.29×10^{-3}	39×10^{-3}
74 "	37.6	0.0114	22.4	2173	0.246	0.0528	76.0	0.1240	7.464×10^{-3}	23×10^{-3}
72 (Activated Alumina sphere)	37.3	0.0108	23.0	2300	0.246	0.0600	78.0	0.119	4.873×10^{-3}	16×10^{-3}
69 "	38.6	0.0101	22.2	1830	0.245	0.0618	103.3	0.1997	1.857×10^{-3}	7×10^{-3}
68 "	38.6	0.0098	22.1	1690	0.245	0.0534	68.5	0.1418	3.678×10^{-3}	13×10^{-3}
67 "	38.3	0.0100	22.2	1698	0.245	0.0546	90.8	0.187	3.678×10^{-3}	13×10^{-3}
53 "	39.9	0.0117	23.5	1970	0.245	0.0666	91.9	0.1650	1.857×10^{-3}	8×10^{-3}
44 "	37.1	0.0121	23.1	1920	0.246	0.04728	91.0	0.1654	1.498×10^{-3}	5×10^{-3}
41 "	37.6	0.0181	27.0	2180	0.248	0.0465	88.9	0.1418	1.857×10^{-3}	5×10^{-3}
32 "	36.8	0.0165	26.0	2390	0.248	0.0468	90	0.1312	4.873×10^{-3}	14×10^{-3}
31 "	37.3	0.0165	26.0	2267	0.248	0.0522	94.8	0.1459	4.873×10^{-3}	16×10^{-3}
30 "	39.2	0.0165	26.3	1750	0.248	0.0444	68.4	0.1360	4.257×10^{-3}	16×10^{-3}
29 "	38.6	0.0175	26.7	2170	0.248	0.0522	84.3	0.1360	4.257×10^{-3}	16×10^{-3}
24 "	41.5	0.0180	28.0	2020	0.248	0.0564	95.0	0.156	3.678×10^{-3}	16×10^{-3}
20 "	37.3	0.0142	22.1	2820	0.247	0.0660	103.0	0.1276	3.678×10^{-3}	16×10^{-3}
16 "	36.2	0.0175	26.3	2920	0.248	0.0522	91.5	0.1086	4.873×10^{-3}	18×10^{-3}
Run 75 (Activated Alumina sphere)	35.4	0.0100	21.4	1490	0.245	0.0378	71.0	0.1678	3.678×10^{-3}	10×10^{-3}

and Mass Transfer of Packed Bed

n	$1-\varepsilon$	a	R_{e0}	Pr	Nu	$\frac{Nu-2}{(Pr)^{1/3}}$	K	H_w	H_2	k_g	Sc	Sh	$\frac{Sh-2}{(Sc)^{1/3}}$	jd
381	0.670	642	621		51.1	53	5.85							
329	0.678	655	607		41.7	43	4.60	0.0238	0.01987	443	0.642	39	43.0	0.060
354	0.627	655	545		41.3	42.5	5.72	0.0206	0.01833	436	0.632	37.8	41.7	0.0667
313	0.707	687	475		38.2	39.1	4.88	0.0197	0.01780	401	0.632	35.4	39.0	0.0710
276	0.698	676	417		39.7	40.8	6.20	0.0204	0.01811	456	0.632	39.2	43.5	0.0900
375	0.840	846	284	0.79	27.6	27.7	5.43	0.01685	0.01573	320	0.628	28.0	30.4	0.0950
398	0.843	846	338	0.791	29.7	30	5.03	0.0174	0.01621	340	0.624	29.7	32.4	0.099
358	0.853	858	244	0.79	28.2	28.4	6.45	0.01725	0.01637	301	0.628	26.2	28.2	0.105
395	0.834	841	348	0.785	34.4	35	6.10	0.01665	0.01558	388	0.628	34.0	37.3	0.0945
95	0.668	421	765	0.790	44.9	46.4	4.03	0.01725	0.01476	283	0.628	45.0	49.5	0.0580
92	0.752	395	762	"	51.2	53.2	5.32							
81	0.787	414	518.5	"	37.4	37.4	4.65	0.01665	0.01470	218	0.628	34.6	38.1	0.066
96	0.760	399	652	"	44.5	46.0	4.65	0.01725	0.01487	272	0.628	44.5	49.7	0.0676
80	0.591	268.5	884	0.789	65	68.2	5.80	0.01760	0.01390	430	0.630	64.2	72.5	0.0692
276	0.600	481	314	0.790	33.5	35.2	6.80	0.01645	0.01433	375	0.628	31.5	34.5	0.1010
948	0.730	914	229	0.790	30.9	31.3	7.85							
143	0.577	308	462	0.793	47.5	49.2	7.10	0.01685	0.01550	388	0.628	49.0	54.7	0.1020
174	0.591	314	635	0.792	50.0	51.8	5.65	0.01780	0.01585	427	0.628	54.0	60.7	0.0824
81	0.581	262.6	765	"	57.7	60.3	5.70	0.01760	0.01455	399	0.628	59.4	66.8	0.0742
425	0.616	494	350	"	35.2	36.0	6.20	0.01750	0.01630	397	0.628	33.2	36.4	0.0910
80	0.574	259.5	640	"	48.8	50.6	5.40	0.01760	0.01444	315	0.628	47.0	52.3	0.0700
141	0.567	305.5	448	"	48.5									
81	0.520	235	680	"	59.7	62.5	6.65	0.01830	0.01543	374	0.628	55.7	62.7	0.0785
344	0.622	482	336	"	40.0	41.1	7.70	0.01725	0.01628	522	0.628	43.5	48.4	0.1220
146	0.575	308	573	"	53.4	55.6	6.90	0.01760	0.01580	390	0.628	51.0	57.2	0.0827
81	0.534	241.8	414	"	43	45.4	7.20	0.01685	0.01480	268	0.628	39.8	44.2	0.0857
115	0.593	310	368	"	32.5	32.2	5.10	0.01673	0.01460	295	0.628	37.2	41.0	0.0975
327	0.618	505	239		27.8	27.9	6.60	0.1725	0.01625	302	0.628	25.2	27.1	0.102
965	0.729	895	165		18.5	17.8	5.25	0.0177	0.01670	373	0.628	20.3	21.4	0.119
8000	0.764	2460	49.9		9.37	7.96	5.87	0.01685	0.01677	468	0.628	9.73	9.00	0.188
1645	0.653	1068	91.1		12.4	11.2	5.07	0.01673	0.01617	306	0.628	12.6	12.4	0.134
1564	0.620	1016	92.0		16.3	15.5	7.10	0.01685	0.01641	353	0.628	14.5	14.6	0.153
8660	0.724	2335	51.3		8.31									
13400	0.935	3760	42.4		6.65	5.02		0.01780	0.0170	380	0.628	6.37	5.10	0.145
8130	0.760	3500	59.9		8.05	6.53								
819	0.706	867	172		21.4	21	6.15	0.02130	0.0204	328	0.638	17.4	17.9	0.1015
1088	0.820	1090	163		22.6	22.3	7.20	0.02130	0.02108	400	0.638	21.6	22.8	0.130
1402	0.569	994	109.3		14.1	13.1	5.15	0.02180	0.02155	336	0.638	15.6	18.1	0.142
1356	0.677	960	173		17.5	16.8	4.52							
2038	0.653	1060	108		17.0									
1822	0.591	956	153		18.4	17.8	5.60	0.01985	0.01936	430	0.638	17.2	17.7	0.113
1012	0.686	827	210		21.4	21.0	5.10	0.02180	0.02125	394	0.638	21.0	22.0	0.100
1200	0.619	1011	80.9		12.7	11.6	5.95	0.0161	0.01546	323	0.628	13.3	13.2	0.159

$$\left. \begin{aligned} j_d &= 1.14 (Re_0)^{-0.45} & Re_0 < 140 \\ j_d &= 0.56 (Re_0)^{-0.305} & Re_0 > 140 \end{aligned} \right\} \quad (5)$$

The ratios of j_h to j_d were 1.05 for lamminar flow and 1.07 for turbulent flow. The results of the authors deviated slightly from the equation obtained by Hougen and coworkers and the critical value for the modified Reynolds number was about 140. The results of the authors on mass transfer data, show agreement with the work of McCune and Wilhelm.

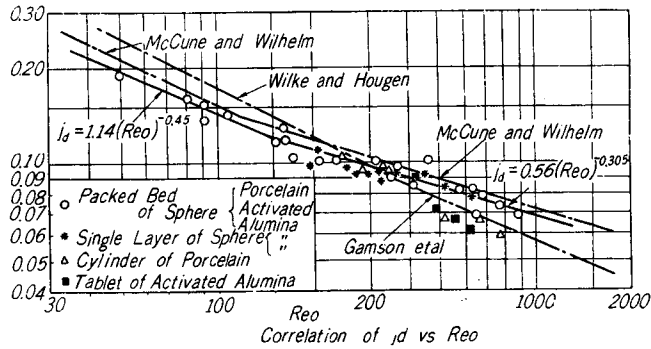


Fig. 5.

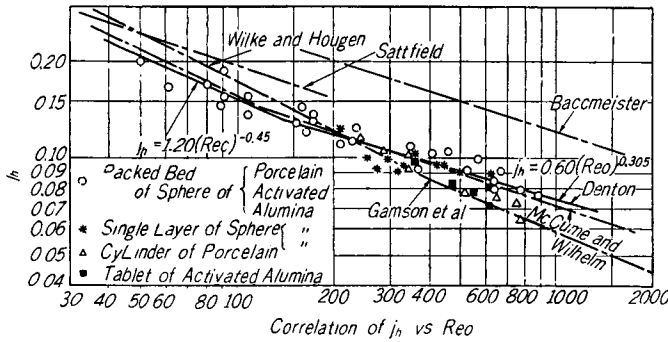


Fig. 6.

(2) Extended interpretation to fluidized beds

The authors did not perform experiments of mass transfer in fluidized beds, but from the experimental data of mass transfer in fluidized beds by McCune and Wilhelm described the value of the voidage, the values of K could be calculated by comparison with equation (2) the same as for packed beds. The calculated results for K in fluidized beds is also plotted against voidage in Fig. 3. The curve for fixed beds was joined smoothly to that for fluidized beds. If the curve is divided into two parts at $1-\epsilon=0.4$, the correlation of heat and mass

transfer for both fixed and fluidized beds may be developed by the following equations along with the variation of K .

$$\left. \begin{aligned} Nu &= 2.0 + 0.113 (KRe_0)^{0.75} (Pr)^{1/3} \\ Sh &= 2.0 + 0.113 (KRe_0)^{0.75} (Sc)^{1/3} \end{aligned} \right\} \quad (6)$$

where

$$\begin{aligned} K &= 4.2 e^{1.75(1-\varepsilon)} & 1-\varepsilon > 0.4 \\ K &= e^{4.37(1-\varepsilon)} & 1-\varepsilon < 0.4 \\ 3000 &> Re_0 > 50 \end{aligned}$$

Acknowledgment

The authors would like to express their appreciation to Mr. Masatoshi Takeuchi to whom they are indebted for the experimental part of this study.

Literature Cited

- 1) Baumeister, E. B., and Bennet, C. O.,: A. I. Ch. E. Journal **4** 67 (1958).
- 2) Denton, W. H.,: "Proceedings of the General Discussion on Heat Transfer" Inst. of Mech. Engrs. (London) p. 370 (1951).
- 3) Gamson, B. W., Thodos, G., and Hougen, O. A.,: Trans. Am. Inst. Chem. Engrs., **39** 1 (1943).
- 4) Hurt, D. W.,: Ind. Eng. Chem., **35** 522 (1943).
- 5) McCune, L. K., and Wilhelm, R. H.,: Ind. Eng. Chem., **41** 1124 (1949).
- 6) Ranz, W. E.,: Chem. Eng. Progr., **48** 247 (1952).
- 7) Ranz, W. E., and Marshall, W. R. Jr.,: Chem. Eng. Progr., **48** 141, 173 (1952).
- 8) Resnick, W. E., and White, R. R.,: Chem. Eng. Progr., **45** 377 (1949).
- 9) Statterfield, C. B., and Resnick, H.,: Chem. Eng. Progr., **50** 504 (1954).
- 10) Wilke, C. R., and Hougen, O. A.,: Trans. Am. Inst. Chem. Engrs., **41** 445 (1945).

Nomenclature

- a : Effective area of heat or mass transfer per unit volume of bed (m²/m³)
- D_p : Particle diameter (m)
- $\left(\frac{dw}{d\theta}\right)_c$: Constant drying rate (kg water/kg-dry mat·hr)
- h : Heat transfer coefficient (kcal/hr m²·°C)
- $(\Delta H)_{im}$: Mean absolute humidity difference of gas transferred, measured from gas stream to the interface (kg-water/kg-dry air)
- j_h : Dimensionless factor for heat transfer
- j_d : Dimensionless factor for mass transfer
- Nu : Nusselt number
- K_G : Mass transfer coefficient (kg/hr·m²·ΔH)
- Pr : Prandtl number
- $Re_0 = \frac{D_p v_0}{\mu}$ Reynolds number

$$Re_p = \frac{D_p v_p}{\mu} \text{ Reynolds number}$$

γ_w : Latent heat (kcal/kg)

Sh : Sherwood number

Sc : Schmidt number

$(\Delta t)_{lm}$: Mean of difference between gas temperature and material temperature ($^{\circ}\text{C}$)

V : Volume occupied by bed (m^3)

v_0 : Velocity of fluid based on cross sectional area of bed (m/sec)

v_p : Average velocity of fluid through the bed (m/sec)

$$K = \frac{v_p}{v_0} = \frac{Re_p}{Re_0}$$

ε : Porosity of bed

μ : Viscosity of fluid (kg/m·sec)